Investigation of Size-Selective $Zr_2@Si_n$ ($n = 16-24$) Caged Clusters

Jin Wang* and Jin Huai Liu

Institute of Intelligent Machines, Chinese Academy of Sciences, Hefei, 230031, AnHui, P. R. China

Received: March 1, 2008; Revised Manuscript Received: March 14, 2008

The size-selective Zr_2Si_n ($n = 16-24$) caged clusters have been investigated by density functional approach in detail. Their geometries, relative stabilities, electronic properties and ionization potentials have been discussed. The dominant structures of bimetallic Zr_2 doped silicon caged clusters gradually transform to Zr_2 totally encapsulated structures with increase of the clustered size from 16 to 24, which is good agreement with the recent experimental result (J. Phys. Chem. A. 2007, 111, 42). Two novel isomers, i.e., naphthalene-like and dodecahedral Zr_2Si_{20} clusters, are found as low-lying conformers. Furthermore, the novel quasi-1D naphthalene-like Zr_nSi_m nanotubes are first reported. The second-order energy differences reveal that magic numbers of the different sized neutral Zr_2Si_n clusters appear at $n = 18$, 20 and 22, which are attributed to the fullerene-like, dodecahedral and polyhedral structures, respectively. The HOMO−LUMO gaps (>1 eV) of all the size-selective Zr_2Si_n clusters suggest that encapsulation of the bimetallic zirconium atoms is favorable for increasing the stabilities of silicon cages.

1. Introduction

Recently, single transition metal (TMA) encapsulated caged silicon cluster have been extensively investigated through theory and experiments because some size-selective $TMA@Si_n$ nanoclusters are indicated as interesting building blocks of self-assembly semiconductor nanomaterials.[1–14] The results suggested that $TMA@Si_n$ nanoclusters had enhanced stabilities and strong size selectivity compared to pure caged silicon cluster. Our previous investigation indicated that the localized site of Zr in $Zr@Si_n$ nanoclusters varied from surface insertion, to concaved occupation, and to total encapsulation in the sealed silicon cage between $ZrSi_8$ and $ZrSi_{16}$.[15] In addition, the stabilization of silicon based cage clusters and nanotubes by encapsulation of transition metal atoms was investigated and the results indicated that metal-encapsulated silicon nanotubes had small conduction gaps and became metallic at infinite length.[16,17] Due to metal encapsulated silicon nanotube including multiple TMAs, it is necessary to investigate encapsulated behaviors of TMA dimer in size-selective caged silicon clusters to obtain their geometries, stabilities and electronic properties in comparison with $Zr@Si_n$ nanoclusters and give the growth mechanism of novel silicon-based nanotubes. Kaya's research group generated Na_2Si_n clusters through laser vaporization and measured their ionization energies.[18] Also, $W_2Si_nH_x^+$ ($n = 8-18$) cationic clusters were observed in external quadrupole static attraction ion trap experiment.[2] Recently, the neutral and charged Si_nNa_p ($n \leq 6$ and $p \leq 2$) clusters have been investigated through DFT approach.[19] Considering that very limited information of dimer TMAs in caged silicon cluster has been obtained in the previous investigations, the geometries, growth behaviors and electronic properties of the novel size-selective $Zr_2@Si_n$ caged cluster have been presently investigated in detail.

2. Computational Details

The geometric optimization of Zr_2Si_n ($n = 16-24$) is performed using the spin unrestricted B3LYP[20,21] combined with an effective core potential LanL2DZ basis sets.[22] The numerous initial Zr_2Si_n isomers are based on a number of known single $TMA@Si_n$ in previous works[6,10,13,15] through adsorption or insertion patterns of Zr_2 in caged silicon clusters.[23] Some optimized structures with high point-group symmetry are suggested as unstable structures corresponding to one or several imaginary vibrational frequencies. Subsequently, these structures are distorted and relaxed along vibrational direction of the imaginary frequency until the true minima are obtained. To test the reliability of the optimization approach, different density functional methods, e.g., B3PW91 and B3P86, are also employed for optimization of some typical candidate of low-lying isomers. The calculated results suggest that the geometries, stabilities and electronic properties of these competitive species are not obviously changed. On the other hand, the previous calculations of $ZrSi_n$ clusters suggested that the calculated values at the (U)B3LYP/LanL2DZ level were in good agreement with those at the (U)B3LYP/GEN level (GEN means 6311+G(d) and LanL2DZ employed for silicon atoms and zirconium atoms, respectively).[15] It is concluded that the calculated results at the unrestricted B3LYP/LanL2DZ level are reliable in the present work. On the basis of the optimized structures of the lowest-energy isomers with different spin states, the results indicate that the spin singlet state of the Zr_2Si_n cluster are the lowest-energy geometries in contrast to spin triplet and quintet states. In addition, to obtain the adiabatic ionization potentials of all the neutral clusters, the geometries of the lowest-energy structure are reoptimized as cationic species. All the calculations are carried out without constraining symmetry by the GAUSSIAN03 program package.[24]

3. Results and Discussion

3.1. Geometries of Size-Selective Zr_2Si_n ($n = 16-24$) Clusters. As shown from the lowest-energy structure 16a in Figure S1, one Zr atom is encapsulated into fullerene-like silicon framework and the other Zr atom occupies the surface site. Also, the previous investigation of $ZrSi_{16}$ suggested that the lowest-energy isomer corresponded to the fullerene-like structure.[15] Compared to the lowest-energy structure 16a, the thermody-

* Author to whom corresponding should be addressed: E-mail: jwang@iim.ac.cn. Fax: +86-551-5592420.

10.1021/jp801828b CCC: $40.75
Published on Web 04/25/2008

namic stability of layered structure 16b is obviously weak compared to the fullerene-like 16a, which is reflected from the total energy of the former being higher than that of the latter by 0.96 eV. A polyhedral isomer 16c is composed of one hexagonal, two rhombic and two pentagonal silicon frameworks. One three-layer stacked isomer 16e is located as a stable structure and the bond length of Zr−Zr (2.958 Å) is smaller than those of the other isomers. Another symmetrical three-layer stacked isomer with C_{2v} point-group symmetry 16f can be described as a double layer hexagonal prism and rhombus; however, the thermodynamic stability of 16f is much weaker than that for16a, which is reflected from the total energy of the former being much higher than that of the latter by 2.56 eV. Additionally, some other amorphous isomers can be also located as minima in the present calculations, whereas their stabilities are quite weak compared to 16a.

In the case of the Zr_2Si_{17} cluster, three kinds of isomers can be found as minima, viz., multilayer stacked structures 17a and 17b, amorphous structures 17c and 17d, and fullerene-like structures 17e and 17f. As shown in Figure S1, the lowest-energy fullerene-like structure 17e of Zr_2Si_{17} is mainly composed of several pentagons. Another low-lying fullerene-like structure 17f is obviously developed from the lowest-energy structure 16a through edge-capping pattern of silicon. It should be noted that the stability of Zr_2 concaved structure 17a or 17b is remarkably weak in comparison with Zr_2 centered and convex structure 17e or 17f. The bond lengths of Zr−Zr in 17a (2.771 Å) and 17b (2.771 Å) are shorter than those of Zr−Zr in 17e (2.999 Å) and 17f (3.174 Å), whereas the averaged bond lengths Zr−Si in 17a and 17b are obviously longer than those in 17e and 17f. This suggests that Zr−Zr interactions in fullerene-like isomers are weakened in contrast to multilayer stacked isomers. On the other hand, the second convex Zr can be efficiently interacted with silicon framework and contributed to forming compact stacked fullerene-like structure 17e and 17f.

As far as the Zr_2Si_{18} caged cluster is concerned, the Zr_2 encapsulated double-layer stacked hexagonal prism 18b is located as minima, whereas its stability is much weaker than fullerene-like 18g and 18h in that its total electronic energy is much higher than those of 18g and 18h by 2.777 and 1.674 eV, respectively. It is suggested that the quasi-1D Zr encapsulated silicon nanotube, which is formed via vertical doping pattern of zirconium atoms in hexagonal prism, is unfavorable. Moreover, the quasi-1D Zr_3Si_{24} nanotube, i.e., triple-layer stacked hexagonal prism, can be optimized to be an unstable structure corresponding to one imaginary vibrational frequency. Relaxation of the vibrational direction of the imaginary frequency leads to one stable structure, which is shown in Figure S1. As seen from the optimized structure of Zr_3Si_{24}, the three zirconium atoms are nonlinear (153.1°) and the silicon hexagonal prismatic cage is obviously distorted, which is similar to Cr_3Si_{24}.[25] In all the located four multilayer stacked structures, only 18b is Zr_2 totally encapsulated structure in comparison with 18a and 18c−e. The lowest-energy isomer 18h, which is described as two pentagonal antiprisms surrounded by nine silicon atoms, is obviously evolved from 17e by addition of extra silicon atom. Similar to size-selective Zr_2Si_n ($n = 16-18$) clusters, different open-caged fullerene-like isomer of Zr_2Si_{19}, which are mainly formed from pentagonal antiprisms, can be found as stable structures. When the size of the cluster increases up to 20, two symmetrical low-lying isomers, i.e., hexagonal prism stacked naphthalene-like isomer 20e with the point-group symmetry (D_{2h}) and dodecahedral isomer 20f, can be located. Similar to dodecahedral $Th@Si_{20}$,[10] the Zr−Zr dimer is encapsulated in the center of the $Zr_2@Si_{20}$ cage. Compared to 20e, the thermodynamic stability of the dodecahedral isomer is slightly strong due to its relatively low total electronic energy. Similar to dodecahedral isomer based on pentagonal prisms, another conformer 20c can be described as eight silicon atoms capping on the hexagonal prism. Analogous to the other size-selective clusters, some different kinds of layer or amorphous structure can be located as minima.

In the case of the Zr_2Si_{21} cluster, the lowest-energy structure 21h is evolved from the dodecahedral Zr_2Si_{20} cluster through insertion of silicon atoms into the pentagonal prism. On the basis of the naphthalene-like Zr_2Si_{20} 20e, one low-lying 21e can be obtained by edge-capping pattern of silicon in hexagonal prism. Additionally, some other different energetic isomers, i.e., fullerene-like and polyhedral isomers, are located as local minima.

When the size of Zr_2Si_n cluster is up to 22, zirconium totally encapsulated silicon cages become dominant and polyhedral 22h is located as the lowest-energy structure. The open-caged isomer 22c can be described as a pentagonal prism surrounded by twelve silicon atoms, and its thermodynamic stability is much weaker than that of the sealed caged polyhedral 22h. A multilayer structure 22f is obviously evolved from Zr_2Si_{21} 21d through insertion of one silicon atom into the hexagonal prism. One high-lying 22a of Zr_2Si_{22} is a zirconium encapsulated double-layer hexagonal prism structure, which is derived from Zr_2Si_{18} 18b by tetracapped silicon atoms.

Similar to Zr_2Si_{22} 22h as the lowest-energy structure, the total electronic energy of Zr_2Si_{23} 23f is obviously lower than those for the other isomers. Different energetic isomers 23b and 23e of Zr_2Si_{23} are obtained from Zr_2Si_{22} 22f and 22g by edge-capping of a silicon atom, respectively. Analogous to Zr_2Si_{22} 22h and Zr_2Si_{23} 23f, polyhedral structure Zr_2Si_{24} 24h is also located as the lowest-energy isomer. The optimized structure of high-lying isomer 24a can be described as ten silicon atoms capped on two heptagonal prisms, which are developed from Zr_2Si_{22} 22f by edge-capped and face-capped silicon atoms in two hexagonal prisms. The total energy of tetracapped Si−Si bioctagonal prism Zr_2Si_{24} 24c is higher than that of polyhedral 24h by 2.39 eV, suggesting that the thermodynamic stability of multilayer 24c is quite weak compared to that of the polyhedral structure. The optimized structure of Zr_2Si_{24} 24f is obviously based on hexagonal and heptagonal prisms surrounded by eleven silicon atoms, whereas its thermodynamic stability is relatively stronger than 24c in that its total electronic energy is much higher than 24 h by 1.37 eV.

Because the naphthalene-like isomer of Zr_2Si_{20} 20f is located as the second lowest-energy isomer and it has a relatively large HOMO−LUMO gap (1.688 eV), the novel assembled zirconium encapsulated silicon nanotubes are considered. Previous investigation suggested that quasi-one-dimensional $TMA_n@Si_m$ can be formed through a TMA vertically doped pattern in the hexagonal prism.[16,17] Herein, one novel assembling pattern, viz., TMAs parallel doped pattern in silicon cages, is considered. When the three units of $ZrSi_{12}$ clusters are stacked as a naphthalene-like pattern, one new symmetrical Zr_3Si_{28} nanotube can be formed. Among the optimized structures, the Zr−Zr bond length (3.455Å) in Zr_3Si_{28} is obviously longer than that (3.175 Å) of Zr_2Si_{20} 20e, whereas the averaged Si−Si bond length (2.385 Å) of Zr_3Si_{28} is shorter than that (2.409 Å) of Zr_2Si_{20} 20e. This suggests that encapsulation of Zr atoms in a hexagonal prism contributes to stacking of silicon cages. Moreover, when the four units of $ZrSi_{12}$ clusters are packed in the naphthalene-like stacking pattern, the nanostructure Zr_4Si_{36} with D_{2h} sym-

TABLE 1: Geometries, Total Electronic Energies, Binding Energies and the Second-Order Energy Difference of the Lowest-Energy Isomers of Zr Cationic$_2$Si$_n$ (n = 16−24) Clusters[a]

cluster	R_{Zr-Zr} (Å)	freq (cm^{-1})	E_T (hartree)	BE (eV)	$\Delta_2E(n)$
$Zr_2Si_{16}^+$	3.058	53.5	−154.9929411	3.020	
$Zr_2Si_{17}^+$	2.993	65.7	−159.1140621	3.044	−0.094
$Zr_2Si_{18}^+$	3.178	61.5	−162.7626815	3.070	0.475
$Zr_2Si_{19}^+$	3.215	50.1	−166.6093539	3.072	−0.378
$Zr_2Si_{20}^+$	2.373	56.1	−170.5106145	3.091	−0.912
$Zr_2Si_{21}^+$	3.085	64.0	−174.4209535	3.147	0.156
$Zr_2Si_{22}^+$	2.877	99.3	−178.3411119	3.206	1.288
$Zr_2Si_{23}^+$	2.915	72.1	−182.2140211	3.208	−1.083
$Zr_2Si_{24}^+$	2.882	89.4	−186.1265298	3.107	

[a] R_{Zr-Zr} enotes the bond length of Zr−Zr; E_T means the total electronic energy of the lowest-energy isomer; BE and $\Delta_2E(n)$ mean the averaged binding energy and the second-order energy difference of the lowest-energy isomer, respectively, freq means the lowest vibrational frequency.

metry is proven to be an unstable structure with one imaginary vibrational frequency. When the symmetry of this structure is decreased, one novel stacked naphthalene-like Zr encapsulated silicon nanotube Zr_4Si_{36}, which has D_2 symmetry, can be located as a stable structure. Therefore, stacking of multiple zirconium atoms doped silicon hexagonal prism as parallel pattern contributes to forming novel naphthalene-like nanotubes. Moreover, the symmetry of this novel nanotube is quite sensitive to the doped numbers of the zirconium atoms.

To sum up, as for the size-selective Zr_2Si_n (n = 16−24) clusters, the dominant geometry gradually varies from the fullerene-like structure to the body-centered polyhedral structure, which is different from the case for the $ZrSi_n$ cluster.[15] Nakajima pointed out that the reactivity of Si_n is generally much lower than that of a metal atom: high and low reactivities correspond to an exterior and an interior metal, respectively; i.e., no obvious reactivity of metal encapsulated can be observed.[26] Compared to the $ZrSi_n$ cluster, the fullerene-like encapsulated structure appears from n = 14 according to the previous calculation results at the UB3LYP/LanL2DZ level,[15] which corresponds to threshold-sized cluster $ZrSi_{14}$ with no reactivity in the recent experiment.[26] As for bimetallic Zr_2 doped silicon clusters, the reactivity is recovered with the doping of the second Zr atom, which appears on the surface of the cluster. The reactivity of Zr_2Si_n toward water is remarkably decreased when the clustered size is larger than 20, and it is implied that the dominant structure transforms to bimetallic Zr_2 encapsulated silicon clusters from that size, which is consistent with our present calculation results.

Initially from the lowest-energy neutral species, the corresponding cationic species are also being reoptimized, suggesting that the Zr−Zr bond length in the silicon cages is sensitive to the size of the cluster and shapes of the silicon cages. As illustrated in Table 1, in the case of polyhedral Zr_2Si_n (n = 22−24), the Zr−Zr bond lengths in cationic species are shorter than those in neutral species, which is different from the situations for the fullerene-like Zr_2Si_n clusters.

3.2. Relative Stabilities of Zr$_2$Si$_n$ Clusters. To predict relative stabilities of the Zr_2Si_n cluster, it is important to calculate the averaged binding energies and the second-order energy difference.

Table 2 and Figure 1 suggest that the averaged binding energies of the size-selective Zr_2Si_n (n = 22−24) are obviously stronger than those of the lower size-selective Zr_2Si_n (n = 16−21) cluster. As mentioned above, the dominant geometry of the Zr_2Si_n cluster is changed from open-caged Zr_2 encapsulated silicon cluster to sealed-caged Zr_2 encapsulated silicon cluster. It can be expected that encapsulation of Zr_2 in the sealed silicon cage efficiently terminates dangling bonds of the silicon cage and increases the stability of the cage.

If a size-selective cluster is abundant in the mass spectrum, the second-order energy difference of this sized cluster is a maximum relative to its neighbors. The quantity denotes the relative stability of Zr_2Si_n atoms compared to clusters of (n + 1) and (n − 1) atoms.

$$\Delta_2(n) = E(n+1) + E(n-1) - 2E(n)$$

As shown in Figure 2, the local maxima can be localized at 18, 20, 22, respectively. The dimer Zr−Zr doped Si_{20} cluster has obvious stability compared to its neighbors, and the lowest-energy structure corresponds to an open-caged dodecahedron. Compared to Zr_2Si_{20}, the extra stability of Zr_2Si_{22} can be ascribed as a zirconium encapsulated polyhedral structure, which is different from Zr_2Si_{18} and Zr_2Si_{20}.

Additionally, sized dependence of the atomic binding energies for the lowest-energy cationic Zr_2Si_n cluster compared to their neutral species are obviously decreased; furthermore, it is suggested that the stabilities of the cationic Zr_2Si_n cluster are weaker than those of neutral clusters. Different from the neutral dodecahedral Zr_2Si_{20}, the relative stability of its corresponding cationic species is weakened compared to its neighbors because its high ionization potential results in ionization of the neutral species, which is not easy and suggests, moreover, that the neutral dodecahedral Zr_2Si_{20} is quite stable so that it could be prepared in the laser vaporization gas-phase experiment.

3.3. Electronic Properties of Zr$_2$Si$_n$ Clusters. To explain the charge transfer mechanism in the Zr_2Si_n cluster, it is necessary to carry out the NBO (natural bonding orbital) analysis and NPA (natural population analysis).[27] As far as the populated charges on doped TMAs in the dominant isomers are concerned, the charges populated on the concaved Zr atom are negative, whereas the charges populated on the convex Zr atom are positive when the size of Zr_2Si_n is between 16 and 18. When the size of the Zr_2Si_n cluster is changed from 18 to 19, all the charges populated on the Zr_2 atoms are indicated to be negative. This suggests that the charge transfer phenomenon between Zr_2 and the silicon cage begins to obviously change, which corresponds to the distribution of the doped bimetals in the silicon cage. In the case of Zr_2 encapsulated silicon caged clusters, the accumulated negative charges on the two zirconium atoms in the Zr_2Si_{20} (−3.198) and Zr_2Si_{22} (−3.249) are obviously higher than those in the Zr_2Si_{21} (−2.484) and Zr_2Si_{23} (−3.091), respectively. It is indicated that the encapsulated zirconium atoms in the caged Zr_2Si_{20} and Zr_2Si_{22} clusters can efficiently dissipate excess negative charge in silicon cage and contribute to the formation of silicon sp^2 hybridization compared to Zr_2Si_{21} and Zr_2Si_{23}. Therefore, the stabilities of Zr_2Si_{20} and Zr_2Si_{22} are obviously stronger than those of Zr_2Si_{21} and Zr_2Si_{23}.

NPA also suggests that the distribution of charges on zirconium atoms is remarkably related to the geometries of the certain sized Zr_2Si_n clusters. For example, the natural charges of Zr_2 atoms in double layer hexagonal prisms Zr_2Si_{18} 18b are suggested as negative charges compared to the lowest-energy fullerene-like isomer Zr_2Si_{18} 18 h.

As far as theHOMO−LUMO gap of the Zr_2Si_{16} cluster is concerned, the lowest-energy fullerene-like Zr_2Si_{16} isomer has obviously a small HOMO−LUMO gap (1.054 eV) compared to the analogous isomer of $ZrSi_{16}$ (2.117 eV).[15] It is suggested that encapsulation of dimer Zr−Zr in a caged silicon cluster distinctly decreases the conduction band gap and increases

TABLE 2: Geometries, Total Electronic Energies, Binding Energies, Second-Order Energy Difference and Ionization Potentials of the Lowest-Energy Isomers of the Neutral Zr_2Si_n ($n = 16-24$) Clusters[a]

cluster	R_{Zr-Zr} (Å)	E_T (hartree)	BE (eV)	$\Delta_2E(n)$	AIP (eV)	VIP (eV)
Zr_2Si_{16}	3.041	−155.2210418	3.357		6.10	6.21
Zr_2Si_{17}	2.999	−159.1140621	3.382	0.169	6.42	6.54
Zr_2Si_{18}	3.091	−163.000869	3.395	0.746	6.48	6.78
Zr_2Si_{19}	3.170	−166.8602686	3.371	−1.002	6.29	6.83
Zr_2Si_{20}	2.507	−170.7564811	3.395	−0.228	6.69	6.98
Zr_2Si_{21}	3.051	−174.6610547	3.427	−0.605	6.42	6.53
Zr_2Si_{22}	2.910	−178.5878737	3.481	1.594	6.61	6.71
Zr_2Si_{23}	2.938	−182.4561085	3.467	−1.159	6.48	6.59
Zr_2Si_{24}	2.895	−186.3669211	3.499		6.42	6.54

[a] R_{Zr-Zr} denotes the bond length of Zr−Zr; E_T means the total electronic energy of the lowest-energy isomer; BE and $\Delta_2E(n)$ mean the averaged binding energy and the second-order energy difference of the lowest-energy isomer, respectively; AIP and VIP mean adiabatic and vertical ionization potentials of the neutral cluster, respectively.

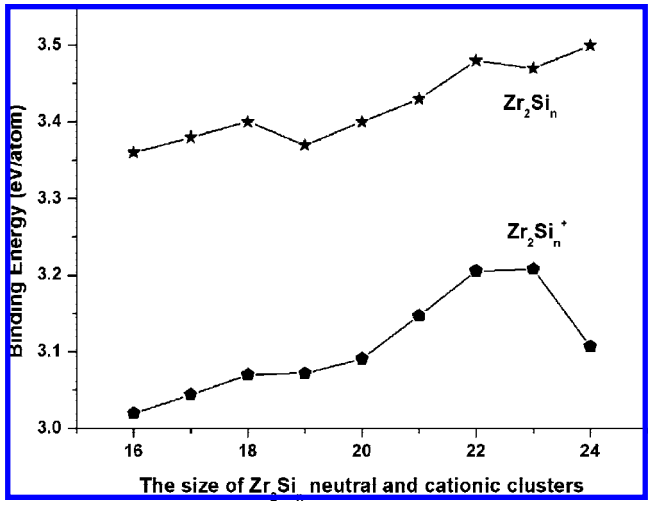

Figure 1. Sized dependence of the averaged atomic binding energies of the neutral and cationic Zr_2Si_n clusters ($n = 16-24$).

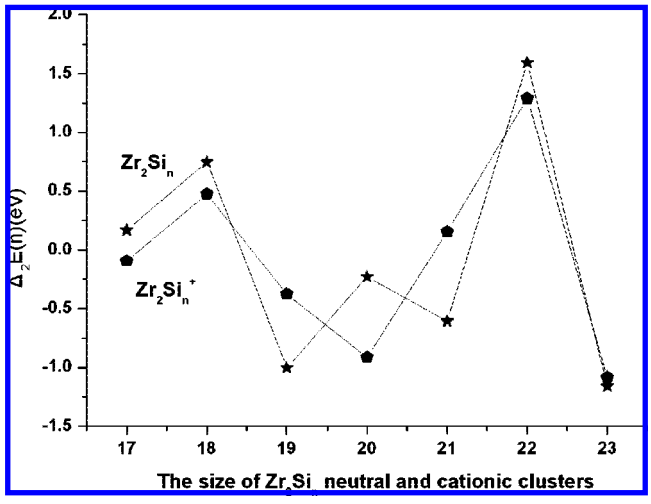

Figure 2. Sized dependence of the second-order energy difference of the neutral and cationic Zr_2Si_n clusters ($n = 16-24$).

metallic properties. As illustrated in Table 3, the HOMO−LUMO gaps of all the endohedral Zr_2Si_n clusters is larger than 1 eV, suggesting that encapsulation of dimer Zr−Zr contributes to increasing the stabilities of silicon cages.

As mentioned before, the novel stacked naphthalene-like zirconium nanotubes can be formed. As far as their HOMO−LUMO gaps are concerned, the gaps gradually decrease with the increase of the number of the encapsulated Zr atoms in silicon cages. In other words, the HOMO−LUMO gap of Zr_4Si_{36} (0.882 eV) is remarkably lower than those of Zr_3Si_{28} (1.592 eV) and Zr_2Si_{20} (1.688 eV). This indicates that these nanotubes become conducting when their lengths increase.

TABLE 3: Nature Charge Population, HOMO−LUMO Gap and Dipole Moment of the Lowest-Energy Isomers of the Neutral Zr_2Si_n ($n = 16-24$) Clusters in all the Located Minima

cluster	natural population	HOMO−LUMO gap (eV)	dipole moment (D)
Zr_2Si_{16}	Zr (1) 0.451 Zr (2) −1.875	1.054	4.421
Zr_2Si_{17}	Zr (1) 0.262 Zr (2) −1.787	1.324	1.538
Zr_2Si_{18}	Zr (1) 0.075 Zr (2) −1.745	1.230	3.655
Zr_2Si_{19}	Zr (1) −0.043 Zr (2) −0.879	1.473	1.638
Zr_2Si_{20}	Zr (1) −1.545 Zr (2) −1.653	1.381	2.342
Zr_2Si_{21}	Zr (1) −0.972 Zr (2) −1.512	1.085	4.897
Zr_2Si_{22}	Zr (1) −1.622 Zr (2) −1.627	1.071	1.837
Zr_2Si_{23}	Zr (1) −1.454 Zr (2) −1.637	1.254	3.107
Zr_2Si_{24}	Zr (1) −1.389 Zr (2) −1.521	1.175	4.028

Electron density surfaces of the different sized Zr_2Si_n clusters are shown in Figure 3. As far as the lowest-energy structures of Zr_2Si_{16} and Zr_2Si_{18} are concerned, the electron density between the second Zr atom and silicon atoms is higher compared to that among adjacent silicon atoms, suggesting strong bonding between the second Zr atom and localized silicon atoms. However, as far as the totally encapsulated lowest-energy dodecahedral Zr_2Si_{20} and polyhedral Zr_2S_{i22} are concerned, electron density between silicon and bimetallic Zr_2 atoms is low, indicating that formation of tight bonding between bimetallic Zr atoms and silicon atoms is unfavorable and covalent bonding between silicon atoms can be formed. As observed from the electron density of the symmetrical naphthalene-like Zr_2Si_{20}, depletion of charges above bihexagonal prisms of dangling bonds with π-bonding characteristics suggests that encapsulated centric Zr atoms efficiently absorb the excess charges in the ring, whereas some charges along Si−Si bond axis remain, meaning that the σ-characteristics state is slightly pulled down within the cage.

The polarity of Zr_2Si_n is obviously correlated with the symmetrical properties of Zr_2Si_n clusters and dangling bonding characteristics of silicon atoms. The stacked naphthalene-like Zr_2Si_{20}, Zr_3Si_{28} and Zr_4Si_{36} are nonpolar molecules due to their symmetries and low dangling bonding properties, whereas the polarity of dodecahedral Zr_2Si_{20} are mainly caused by existence of dangling bonds of some silicon atoms.

3.4. Ionization Potential Energies of Neutral Zr_2Si_n Clusters. On the basis of the lowest-energy structure of different sized neutral Zr_2Si_n cluster, the cationic Zr_2Si_n clusters are also calculated at the same level.

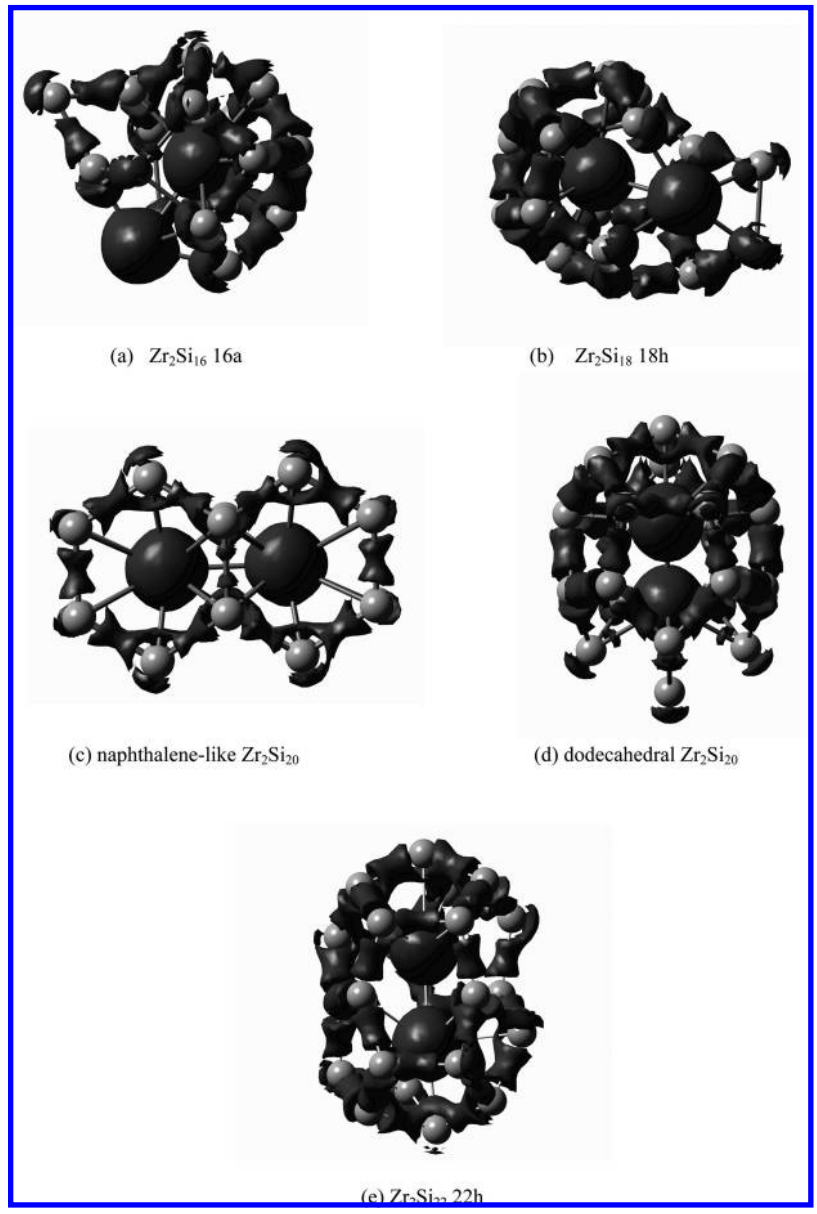

Figure 3. Constant electronic charge density surfaces for (a)−(e) the lowest-energy isomer of Zr_2Si_{16}, Zr_2Si_{18}, naphthalene-like and dodecahedral Zr_2Si_{20}, Zr_2Si_{22}. The charge densities at the surface are 0.060 au.

The adiabatic and vertical ionization potential energies can be calculated by the following formula:

$$\mathrm{AIP} = E_T(\text{optimized } Zr_2Si_n^+) - E_T(\text{optimized } Zr_2Si_n)$$

$$\mathrm{VIP} = E_T(Zr_2Si_n + \text{with neutral geometry}) + E_T(\text{optimized } Zr_2Si_n)$$

According to the results of total electronic energies of the lowest-energy neutral clusters and its corresponding cationic clusters, the ionization potential energy of the different sized Zr_2Si_n cluster can be obtained. As shown in Figure 4 and Table 2, the AIP (adiabatic ionization potential energy) of Zr_2Si_{20} (6.69 eV) and Zr_2Si_{22} (6.61 eV) is obviously larger than those of the other sized cluster, suggesting that the neutral Zr_2Si_n (n = 20 and 22) clusters are relatively more stable in ionization pathway than the other sized clusters, which is consistent with the results of the averaged binding energy and second-order energy difference of the neutral species. It should be pointed out that the geometric rearrangements between the neutral and cationic clusters lead to some deviation between the AIP and VIP values. For example, in the case of Zr_2Si_{19} cluster, the difference (0.54 eV) between the AIP and VIP values is dramatically large compared to the other sized clusters. As seen from the optimized structure of cationic $Zr_2Si_{19}^+$ cluster, the interdistance of Zr−Zr (3.215 Å) is much longer than that of Zr−Zr (3.170 Å) in neutral species, indicating that geometric rearrangement causes obvious deviation between AIP and VIP.

4. Conclusions

The geometries, relative stabilities, electronic properties and ionization potential energies of size-selective Zr_2Si_n (n = 16−24) caged clusters are investigated using UB3LYP/LanL2DZ approach. All of the results are summarized as follows:

(1) Numerous isomers of the size-selective Zr_2Si_n (n = 16−24) clusters suggest that the dominant structures can be transformed from fullerene-like to polyhedral isomers. When the size of the caged Zr_2Si_n cluster is lower than 20, the second

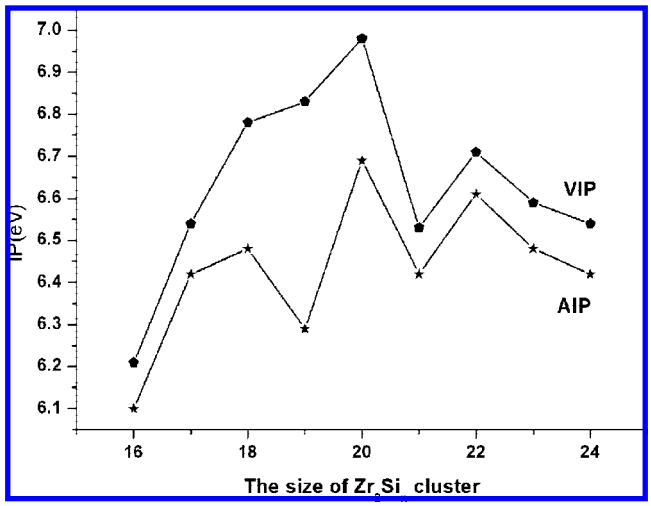

Figure 4. Sized dependence of the vertical and adiabatic ionization potentials (VIP and AIP) of the lowest-energy isomers of neutral and cationic Zr_2Si_n ($n = 16-24$) clusters in all the located minima

zirconium atom mainly occupies the surface adsorption site of the silicon cage, whereas the second zirconium atom begins to be concave in silicon cages at $n = 20$, resulting in formation of the symmetrical dodecahedral isomers. It should be mentioned that if the size of Zr_2Si_n is higher than 21, the dominant geometry can be described as irregular polyhedrons. Novel stacked naphthalene-like Zr_2Si_{20} with point-group symmetry D_{2h} is located as the low-lying isomer, suggesting that formation of novel quasi-1D naphthalene-like zigzag Zr_nSi_m nanotubes is possible. Moreover, the stable short naphthalene-like zigzag Zr_3Si_{28} and Zr_4Si_{36} nanotubes can be located for the first time.

(2) Natural population analysis of the lowest-energy isomer of every sized cluster indicates that charge reversible transferring from silicon cages to all the two zirconium atoms obviously occurs at Zr_2Si_{20}, which is related to the occupied site of zirconium atoms in silicon cages.

(3) The averaged binding energies of the size-selective Zr_2Si_n ($n = 22-24$) are obviously stronger than those of the lower sized Zr_2Si_n ($n = 16-21$) cluster. Compared to neutral species, their corresponding cationic species have relatively low binding energies indicating that their stabilities are weak. As far as the magic numbers of neutral caged Zr_2Si_n clusters are concerned, the magic numbers of relative stabilities are 18, 20 and 22 according to analysis of the second-order energy difference. It should be mentioned that fullerene-like, dodecahedral and polyhedral cages contribute to formation of special stabilities of Zr_2Si_{18}, Zr_2Si_{20} and Zr_2Si_{22} compared to their neighbors.

(4) The HOMO−LUMO gaps of the encapsulated Zr_2Si_n caged clusters are larger than 1 eV, suggesting that encapsulation of Zr_2 is favorable to increase the stabilities of the large sized caged silicon clusters. Accompanied by an increase of the lengths of the novel stacked naphthalene-like zirconium silicon nanotubes, the HOMO−LUMO gaps gradually decrease, suggesting that these nanotubes conducting behaviors become to be strengthened.

(5) The dipole moments of the novel quasi-1D naphthalene-like zigzag Zr_nSi_m nanotubes are zero, indicating that these nanotubes are symmetrical and characteristics of dangling bonds in silicon cages are dramatically weakened. Furthermore, the termination of dangling bonds of naphthalene-like Zr_nSi_m nanotubes is favorable for enhancing their stabilities. In the case of the novel dodecahedral Zr_2Si_{20}, although the distribution of Zr−Zr in the silicon cage is symmetrical, the dangling bonding characteristics of the bottom silicon atoms can still cause its polarity.

(6) The ionization potential of dodecahedral Zr_2Si_{20} is the highest in all the different sized clusters, suggesting that the neutral dodecahedral Zr_2Si_{20} cluster is relatively more stable in ionization pathway in comparison with the other sized clusters and could be observed in laser-vaporization gas-phase experiments.

Acknowledgment. This work is supported by National Key Fundamental Research Development Plan of China (2007 CB 936603) and National Nature and Science Foundation of China (60574094).

Supporting Information Available: Equilibrium geometries of the Zr_2Si_n ($n = 16-24$) clusters. Equilibrium geometries of Zr_3Si_{28} and Zr_4Si_{36} quasi-1D naphthalene-like nanotubes. This material is available free of charge via the Internet at http://pubs.acs.org.

References and Notes

(1) Beck, S. M. *J. Chem. Phys.* **1987**, *87*, 4233. (a) Beck, S. M. J. *Chem. Phys.* **1989**, *90*, 6306.
(2) Hiura, H.; Miyazaki, T.; Kanayama, T. *Phys. Rev. Lett.* **2001**, *86*, 1733. Miyazaki, T.; Hiura, T.; Kanayama, T. *Phys. Rev. B.* **2002**, *66*, 121403.
(3) Ohara, M.; Koyasu, K.; Nakajima, A.; Kaya, K. *Chem. Phys. Lett.* **2003**, *371*, 490.
(4) Khanna, S. N.; Rao, B. K.; Jena, P. *Phys. Rev. Lett.* **2002**, *89*, 016803.
(5) Sporea, C.; Rabilloud, F. J. *Chem. Phys.* **2007**, *127*, 164306.
(6) Kawamura, H.; Kumar, V.; Kawazoe, Y. *Phys. Rev. B* **2004**, *70*, 245433.
(7) Mpourmpakis, G.; Froudakis, G.; Andriotis, A. N.; Menon, M. *Phys. Rev. B* **2003**, *68*, 125407.
(8) Kawamura, H.; Kumar, V.; Kawazoe, Y. *Phys. Rev. B* **2005**, *71*, 075423.
(9) Lu, J.; Nagase, S. *Phys. Rev. Lett.* **2003**, *90*, 115506.
(10) Singh, A. K.; Kumar, V.; Kawazoe, Y. *Phys. Rev. B* **2005**, *71*, 115429.
(11) Kumar, V.; Majumder, C.; Kawazoe, Y. *Chem. Phys. Lett.* **2002**, *363*, 319.
(12) Kumar, V.; Singh, A. K.; Kawazoe, Y. *Phys. Rev. B* **2006**, *74*, 125411.
(13) Kumar, V.; Briere, T. M.; Kawazoe, Y. *Phys. Rev. B* **2003**, *68*, 155412.
(14) Jaeger, J. B.; Jaeger, T. D.; Duncan, M. A. *J. Phys. Chem. A* **2006**, *110*, 9310.
(15) Wang, J.; Han, J. G. J. *Chem. Phys.* **2005**, *123*, 064306.
(16) Andriotis, A. N.; Mpourmpakis, G.; Froudakis, G.; Menon, M. N. *J. Phys.* **2002**, *4*, 78–1.
(17) Mpourmpakis, G.; Froudakis, G. E.; Andriotis, A. N.; Menon, M. J. *Chem. Phys.* **2003**, *119*, 7498.
(18) Kishi, R.; Iwata, S.; Nakajima, A.; Kaya, K. *J. Chem. Phys.* **1997**, *107*, 3056.
(19) Sporea, C.; Rabilloud, F.; Allouche, A. R.; Frécon, *J. Phys. Chem. A* **2006**, *110*, 1046.
(20) Becke, A. D. *Phys. Rev. A* **1988**, *38*, 3098.
(21) Lee, C.; Yang, W.; Parr, R. G. *Phys. Rev. B* **1988**, *27*, 785.
(22) Wadt, W. R.; Hay, P. J. J. *Chem. Phys.* **1985**, *82*, 284.
(23) Yoo, S.; Zeng, X. C. *J. Chem. Phys.* **2005**, *123*, 164303.
(24) Frish, M.; et al. *Gaussian03*; Gaussian Inc.: Pittsburgh, PA, 2003.
(25) Kumar, V.; Kawazoe, Y. *Phys. Rev. Lett.* **2003**, *90*, 055502.
(26) Kayasu, K.; Atobe, J.; Akutsu, M.; Mitsui, M.; Nakajima, A. J. *Phys. Chem. A* **2007**, *111*, 42.
(27) Glendening E. D.; Reed, A. E.; Carpenter, J. E.; Weinhold, F. *NBO 3.0 Program Manual, Theoretical Chemistry Institute and Department of Chemistry*; University of Wisconsin: Madison, WI 53706.

JP801828B